ELSEVIER

Biochimica et Biophysica Acta 1373 (1998) 1–16

BIOCHIMICA ET BIOPHYSICA ACTA

BBA

Fluorescence quenching data interpretation in biological systems The use of microscopic models for data analysis and interpretation of complex systems

Miguel A.R.B. Castanho [a,b,*], Manuel J.E. Prieto [a]

[a] *Centro de Química Física Molecular, Complexo I - IST, P-1096 Lisbon Codex, Portugal*

[b] *Departamento de Química e Bioquímica da FCUL, Campo Grande, Ed. C1-5º, P-1700 Lisbon, Portugal*

Received 13 January 1998; revised 5 May 1998; accepted 6 May 1998

Abstract

In micro-heterogeneous media (e.g. membranes, micelles and colloidal systems), the fluorescence decay in the absence of quencher is usually intrinsically complex, e.g. due to the existence of several sub-populations with different micro-environments. In this case it is impossible to analyze data in detail (accounting for transient effects) and simpler formalisms are needed. The objective of the present work is to present and discuss such simpler formalisms. The goal is to achieve simple data analysis and meaningful, clear data interpretation in complex systems using microscopic models that consider several sub-populations of chromophores. Two points are dealt with in detail. (i) It is shown that the approximation of the transient effects by the quenching sphere-of-action model is not always possible. The quenching sphere-of-action concept can be regarded as a valuable tool, although crude, only in a limited range of experimental conditions, namely time resolution. (ii) The Stern-Volmer equation usually used for data analysis is only valid for a limited range of small and moderate equilibrium association constants, K_a, although this is frequently overlooked in the literature. Self-consistency criteria are presented for the proposed methods. The well-known downward curvature due to a fraction of fluorophores which is not accessible to the quencher is only a limiting case from a set of possible situations which result in deviations to linearity. A systematic classification of the different types of quenching is presented.

Keywords: Fluorescence; Quenching; Analysis; Diffusion

1. Introduction

The use of the Smoluchowski equation (for a review see e.g. [1]) to interpret the Stern-Volmer plots in fluorescence quenching is a usual methodology to obtain information on the structure and dynamics of several compounds, including many species of biological interest, in a great variety of homogeneous and micro-heterogeneous (e.g. micelles and membranes) media. Nevertheless, this methodology can only be applied to very simple systems, from both the molecular (e.g. only one, homogeneous, population of both fluorophores and quenchers) and kinetic points of view. Therefore several alterations have been introduced in this methodology to enable its application to more complex systems. The most common ones, for instance, consider heterogeneous populations of fluorophores and interactions involving

* Corresponding author. Fax: +351 (1) 8464455; E-mail: pcmcastanho@alfa.ist.utl.pt

0005-2736/98/$19.00
PII: S0005-2736(98)00081-9

the fluorophores in the ground state and quenchers. Increased kinetic complexity includes reaction-controlled processes and specific reaction schemes. These kinds of improvements are spread over the literature and relevant reviews on the application of fluorescence quenching data analysis to complex systems (such as the biochemical systems) have been published in the last years, namely by Laws and Contino [2] dedicated to microscopic models, and by Eftink and Ghiron [3] dedicated mainly to kinetic models to study protein fluorescence quenching.

Lehrer [4] rationalized downward deviations to linear Stern-Volmer plots of protein fluorescence quenching by iodide, considering that a fraction of the total chromophore population was 'protected', unable to contact with iodide due to its location in hydrophobic pockets of the proteins. Thus, the light emitted by these fluorophores is independent of the concentration of the quencher, causing the mentioned downward deviation to linearity. Eftink and Ghiron [5] discuss Stern-Volmer plots having upward deviations to linearity caused by heterogeneities in the quencher concentration and some restrictions in the accessibility of the fluorophores by the quenchers. Owen and Vanderkooi [6] predict negative deviations to linearity due to the diffusion of the quencher in heterogeneous media before reaching the chromophore. Slight deviations to linearity in Stern-Volmer plots (in both steady and transient states) are a consequence of the so-called transient effects in the Smoluchowski formulation, which was later modified by Collins and Kimball (e.g. [7]).

In this work, a global approach accounting for several of these interpretations is looked for. The goal is to be able to interpret non-linear Stern-Volmer plots in complex systems in a generalized and simple way that involves the combination of time-resolved and steady-state data. Particular attention is devoted to the quenching sphere-of-action model [8] due to its ubiquitous utilization and fame, which result from its simple and intuitive basic concepts.

2. Theoretical background

One possible approach to the dynamic (i.e. diffusion-dependent) fluorescence quenching quantification involves Fick's diffusion equation solution. The basic idea is to calculate the concentration gradient of the quencher species, Q, around a central pool that gathers all the fluorophores population (for more details see e.g. [9]). The quenchers cannot get closer to this pool by less than distance R_{FQ} (the maximum approach distance). The assumptions are that fluorescence quenching is started at the instant of excitation by light and the process is not reversible. The rate of diffusion of Q into the central pool influences the quenching process velocity (see later). These are important assumptions regarding the boundary conditions applied to the solution of Fick's equation.

There are two limit cases of great relevance for the clear understanding of fluorescence quenching.

(1) In one of these limits, the quenching reaction itself occurs in a time-scale smaller than the one necessary for significant diffusion. This is the case compatible with the boundary conditions used by Smoluchowski (e.g. [6]): The concentration of Q at the distance of maximum approach, R_{FQ}, is zero for $t>0$. The reaction velocity is limited only by the rate of Q reaching the surface of the shell at distance R_{FQ} from the pool, reacting. This is the so-called diffusion-controlled limit. The reaction rate is named k_d and is equal to:

$$k_d = 4\pi R_{FQ} D_{FQ} \quad (1)$$

(D_{FQ} is the mutual diffusion coefficient, i.e. is the sum of both Q and fluorophore diffusion coefficients) for neutral species.

(2) The other limit is the opposite of the first one: the reaction is much slower than diffusion leading to a completely diffusion-independent process.

Therefore, a reaction probability between 0 and 1 is to be considered when a Q species (molecule, atom, ion or radical) reaches R_{FQ}. The reaction velocity is dependent on the diffusion of Q but not exclusively. The central pool decreases the concentration of Q at the R_{FQ} shell relative to instant zero and a gradient of species Q is formed around the central pool. The reaction probability, however, is not unit and therefore the concentration of Q at R_{FQ} is never zero.

A steady state is reached some time after instant zero, when the rate of reaction is compensated by the flux of Q that results from its concentration gradient

around the central pool. The fact that the steady state is not instantaneously achieved leads to some peculiarities in fluorescence quenching, generally named 'transient effects'.

The transition between these two limits can be described by means of the following boundary condition: the fluorescence quenching velocity is now proportional to the concentration of Q in the spherical shell of radius R_{FQ}. This is the radiation boundary condition (named this way due to its application in the heat diffusion) proposed by Collins and Kimball (for a review see e.g. [1]). It should be recalled that Smoluchowski considered the reaction velocity to be proportional to the rate of collision of one of the reactants with the surface border of the central pool.

According to Collins and Kimball, the time dependence of the bimolecular reaction constant is:

$$k(t) = \frac{k_d k_a}{k_d + k_a}\left\{1 + \frac{k\mathrm{a}}{k_d}\exp\left[\frac{D_{FQ}t}{R_{FQ}^2}\left(1 + \frac{k_a}{k_d}\right)^2\right]\right.$$

$$\left.\mathrm{erfc}\left[\frac{\sqrt{\mathrm{D_{FQ}t}}}{\mathrm{R_{FQ}}}\left(1 + \frac{\mathrm{k_a}}{\mathrm{k_d}}\right)\right]\right\} \quad (2)$$

(k_a would be the reaction constant if the diffusion was infinitely fast and k_d is the Smoluchowski limit, $k_d = 4\pi R_{FQ} D_{FQ}$).

Nevertheless, Eq. 2 is not easy to deal with and a simplified version which results from $\exp(x^2)\mathrm{erfc}(x) \approx 1/(x\sqrt{\pi})$, usually named the 'long-time' approximation, is considered:

$$k(\mathrm{t}) = \frac{k_d k_a}{k_d + k_a}\left(1 + \frac{k_a \quad R_{FQ}}{k_d + k_a\sqrt{\pi D_{FQ}t}}\right) \quad (3)$$

In the typical experimental conditions usually found in solution ($D_{FQ} \approx 10^{-5}$ cm^2 s^{-1}, $R_{FQ} \approx 0.5$ nm and $k_a \approx k_d$), Eq. 3 is a good approximation only for $t > 50$ ps. However, in viscous media such as membranes, micelles or colloidal systems, Eq. 3 holds as a good approximation for t higher than a few ps (see discussion in the Appendix of reference [10]). A quest for an operational $k(t)$ equation valid in a very broad time range has been successfully undertaken by several workers (e.g. [11,12]). This problem will be addressed later.

Two other points deserve attention. (i) Most of the heterogeneous systems cannot be considered to be infinite in size and/or have reduced dimensionality. If, for instance, a membrane was strictly bidimensional, different boundary conditions for the Smoluchowski formalism should be applied [13]. The best approach to the specific situation of probe diffusion in a membrane is the one used by Owen [14], in which the finite bilayer width is considered (cylindrical geometry). Owen [14] introduced a parameter which defines the transition instant from spherical (3D) to the cylindrical geometry. This value is longer than the lifetime of most of the fluorescent probes. In agreement, Almgren [15], in a comparative study of quenching in restricted dimensionality, states that deviations from 3D occur only for very long fluorescence lifetimes.

2.1. Phenomenological approach

A phenomenological approach can be very useful for the understanding of the processes we are describing (e.g. [16]). Consider the kinetic scheme relative to the irreversible reaction between A and B:

$$\mathrm{A} + \mathrm{B} \overset{k_{-d}}{\underset{k_d}{\rightleftharpoons}} (\mathrm{AB}) \xrightarrow{k_a} \mathrm{P} \quad (4)$$

($k_{i=-d,d,a}$ are the constants of each of the indicated processes). The Smoluchowski limit is verified for $k_a \gg k_d$. Therefore, in this limit, it is a process uniquely controlled by the diffusion of species A and B. So, the kinetic constant for the fluorescence quenching process (where A and B are the fluorophore, F, and quencher, Q), k_q, in steady-state conditions is

$$k_q = k_d = 4\pi N_A R_{FQ} D_{FQ} \quad (5)$$

(N_A is Avogadro's constant, R_{FQ} and D_{FQ} are the sum of the molecular radii and diffusion coefficients of fluorophore and quencher, respectively), this equation being similar to Eq. 1. If k_a and k_d are comparable, a similar situation to the one studied by Collins and Kimball is obtained. The process is not only diffusion-controlled but also reaction-controlled. This reaction control was interpreted in its simpler formulation: the collisions between F and Q do not always result in quenching. The Smoluchowski equation has to be modified, including an efficiency parameter, γ:

$$k_q = \gamma 4\pi N_A R_{FQ} D_{FQ} \quad (6)$$

which is

$$\gamma = \frac{k_a}{k_a + k_{-d}} \quad (7)$$

The steady-state equation derived from the RBC formalism is equal to Eq. 6 [16]. Sometimes, Eq. 6 is rewritten and presented in the form:

$$k_q = 4\pi N_A(\gamma R_{FQ}) D_{FQ} = 4\pi N_A R_{FQ,ef} D_{FQ} \quad (8)$$

and $R_{FQ,ef}$ is the so-called effective radius. The reason for this kind of presentation is purely intuitive: fewer reactive molecules should get closer in order to react. This could lead to an effective radius very small as compared to R_{FQ}, i.e. without direct physical meaning. A correct analysis implies the determination of γ, as discussed later, avoiding the effective radius concept. Certainly the correct approach is to keep γ to describe the intrinsic reaction efficiency as previously described.

2.2. Fluorescence intensity decay

Nemzek and Ware [10], based on the radiation boundary condition, described a decay law for a fluorescent species in the presence of a quencher concentration [Q], in 3D:

$$I(t) = I(0)\exp\left[-\frac{t}{\tau_0} - 4\pi R'_{FQ} D_{FQ} N_A [Q] t\left(1 + \frac{2R'_{FQ}}{\sqrt{\pi D_{FQ} t}}\right)\right] \quad (9)$$

where R'_{FQ} is closely related to $R_{FQ} \times k_a/(k_a+k_d)$ and τ_0 is the fluorescence lifetime for $[Q]=0$. Eq. 9 is valid in the same time range as Eq. 3: it is valid only for data analysis in solution in the time range $t > 50$ ps, which is more than the time resolution available with modern laser systems. In viscous media such as membranes, micelles and colloids, Eq. 3 holds for very short times. The processes that originate the term dependent on $\sqrt{t}$ in Eq. 9 are generally referred to as the transient effects. Integration leads to the steady-state Stern-Volmer equation:

$$\frac{I_{f,0}}{I_f} = (1 + 4\pi R_{FQ} D_{FQ} N_A [Q] \tau_0)\, Y^{-1} \quad (10)$$

where I_f and $I_{f,0}$ are the fluorescence intensities at Q concentrations [Q] and 0, respectively, and:

$$Y = 1 - \frac{\beta}{\sqrt{\alpha}}\sqrt{\pi}\exp\left(\frac{\beta^2}{\alpha}\right)\mathrm{erfc}\left(\frac{\beta}{\sqrt{\alpha}}\right) \quad (11)$$

$$\alpha = \frac{1}{\tau_0} + 4\pi R'_{FQ} D_{FQ} N_A [Q] \quad (12)$$

$$\beta = 4R'^2_{FQ}\sqrt{\pi D_{FQ}} N_A [Q] \quad (13)$$

$$\mathrm{erfc}\left(\frac{\beta}{\sqrt{\alpha}}\right) = \frac{2}{\sqrt{\pi}}\int_{\beta/\sqrt{\alpha}}^{\infty} e^{-u^2} du \quad (14)$$

The function Y is not easy to deal with and its approximation by an exponential function can be performed within a range of $\beta/\sqrt{\alpha}$ with a certain error. When x approaches zero, $\ln(Y^{-1}(x)) \approx x\sqrt{\pi}$, i.e.,

$$Y^{-1}\left(\frac{\beta}{\sqrt{\alpha}}\right) \approx \exp\left(\frac{\beta\sqrt{\pi}}{\sqrt{\alpha}}\right) \quad (15)$$

But,

$$\frac{\beta}{\sqrt{\alpha}} = \frac{4R'^2_{FQ}\sqrt{\pi D_{FD}} N_A [Q]}{\sqrt{\frac{1}{\tau_0} + 4\pi R'_{FQ} D_{FQ} N_A [Q]}} \quad (16)$$

and the denominator can be approximated to $1/\sqrt{\tau}$, where τ is the fluorescence lifetime in the presence of quencher, ignoring transient effects. Therefore,

$$\frac{\beta}{\sqrt{\alpha}} = 4R'^2_{FQ}\sqrt{\pi\tau D_{FQ}} N_A [Q] \quad (17)$$

and

$$Y^{-1}\left(\frac{\beta}{\sqrt{\alpha}}\right) \approx \exp(4R'^2_{FQ}\pi\sqrt{\tau D_{FQ}} N_A [Q]) \quad (18)$$

The exponential argument in Eq. 18 is usually presented as $V' N_A [Q]$, where

$$V' = 4\pi R'^2_{FQ}\sqrt{D_{FQ}\tau} \quad (19)$$

has the units of volume. Combining Eqs. 10,18,19,

$$\frac{I_{f,0}}{I_f} \approx (1 + K_{SV}[Q])\exp(V' N_A [Q]) \quad (20)$$

K_{SV} is named the Stern-Volmer constant, $K_{SV} = 4\pi R'_{FQ} D_{FQ} N_A [Q] \tau_0$.

Eq. 20 has a central role in this work because it is

used very often in the literature and its limitations and interpretation are overlooked most of the time. In fact, Eq. 20 was already used before the Nemzek and Ware formulations. Weller [17] named V' the molar volume of diffusion. In this work it will be shown that V' is related to the sum of the volumes that the fluorophore occupies in its random walk during the time τ. For many elementary steps in 3D this sum of volumes would be equivalent to a sphere.

We have just detailed how the transient term can be approximated to an exponential (Eq. 20). As we described, the time range of validity encompasses in viscous media the time resolution of modern instrumentation (ps). Moreover, Periasamy et al. [18] have shown that a better equation (i.e. valid even for shorter times) than the one of Nemzek and Ware (Eq. 9) should include an exponential decrease of I_0. This exponential would add to the one previously described (Eq. 20).

2.3. The quenching sphere-of-action

An analogous equation to Eq. 20 can be obtained from very simple and intuitive assumptions on the microscopic level of the quenching process. This is widely known as the quenching sphere-of-action model (based on the formulations of F. Perrin [19] and having a generalized form, involving diffusive and reactional control presented in [17]). Imagine fluorophore and quencher random distributions at the instant of excitation. There is a certain probability (that in most experimental conditions can be expected to be described by Poisson distribution) that at this instant, some fluorophore and quencher molecules are in contact. Fluorophore molecules in contact with the quencher at the instant of excitation will not fluoresce. At best, they have a non-unit probability of fluorescing, γ, if the quenching reaction is not totally efficient. Some of the other chromophores will be quenched in a diffusion dependent manner. This leads to [20]:

$$\frac{I_{f,0}}{I_f} = (1 + k_q[Q]\tau_0)\exp(\gamma V N_A[Q]) \quad (21)$$

where k_q is as defined in Eq. 6 and V is the sphere-of-action volume, i.e. the volume of the sphere that surrounds the chromophore within which the quencher can be considered to be in contact with the chromophore. Obviously, the radius of this sphere is the distance of closest approach, R_{FQ}. Although Eq. 21 is deduced assuming F and Q as point molecules, it holds for non-point molecules to a good approximation because the probability of finding one quencher molecule inside the sphere-of-action is very close to the probability of finding at least one molecule inside the sphere-of-action (i.e. excluded volume effects are negligible).

Eq. 21 can be rewritten for the simplest case ($\gamma = 1$):

$$\frac{I_{f,0}}{I_f} = (1 + K_{SV}[Q])\exp(V N_A[Q]) \quad (22)$$

The formal similarity between Eqs. 20,22 is obvious. The question is, what is the relation between V' and V? Weller [17] suggested an intuitive interpretation for V' that is not far from the notion of V, but can V' be seen as the volume of a sphere with radius R_{FQ}, surrounding the chromophore? In more general terms, how can the transient terms in the Nemzek and Ware formulation be related to the quenching sphere-of-action model? This is the question we will try to answer in order to establish a simple methodology to interpret non-linear Stern-Volmer plots in complex systems. As described, the complexity of Eq. 9 prevents its application in heterogeneous systems. At variance, Eqs. 20,22 are simple.

2.4. The physical meaning of V'

Following Weller's suggestion, we can try to relate V' to the volume of diffusion. The first approach is to consider the sum of volumes successively occupied by the fluorophore in its random walk starting from the instant of excitation. The simplest way is to conveniently transform Eq. 19, leading to Eq. 23 (in 3D),

$$V' = \frac{4\sqrt{n}}{n\sqrt{6}}\pi R_{FQ}^2 n\sqrt{6D_{FQ}\Delta\tau} = \sqrt{\frac{16}{6n}} n V_c \quad (23)$$

V_c is the volume of the cylinder with radius R_{FQ} and length $\sqrt{6D_{FQ}\Delta\tau}$. $\Delta\tau$ is the time it takes to the fluorophore to complete one elementary step in its random walk and n is the total number of elementary steps during the period τ. The physical meaning

comes from the fact that this length is the distance covered by the fluorophore in the elementary step of the random walk, i.e. nV_c is the total sum of volumes occupied by the fluorophore during the excited state period, τ. So, the concept of V' should be critically analyzed. V' only approximates nV_c for one to three elementary steps. Such interpretation is so restricted (see later) that it is virtually meaningless. Another way has to be followed. We looked for a relation between V, a parameter with an immediate physical meaning, and V'. What are the conditions in which the volume V' can be interpreted as V?

The reader should recall that D_{FQ} is the mutual diffusion coefficient, so it is no different to consider static (relative to the lab. frame coordinates) fluorophores and diffusing quenchers with D_{FQ} (as Smoluchowski did) or vice versa (as we will use from now on for the sake of simplicity).

When $n \to \infty$ and as long as $r \ll nl$ (r is the initial to end distance in a random walk process and l is the elementary step length), which is an almost universal condition [21], the probability that the end position (i.e. at instant τ) is at a distance between r and $r+dr$ from the initial position (i.e. at instant zero) is:

$$\omega(r)dr = \left(\frac{B}{\sqrt{\pi}}\right)^3 \exp(-B^2r^2)4\pi r^2 dr \quad (24)$$

$$B = \frac{1}{l}\sqrt{\frac{3}{2n}} \quad (25)$$

The root mean square of this distribution is related to the root mean square 'pseudo-radius-of-gyration' (i.e. the radius of gyration that would have a chain linking all the intermediate positions of the chromophores during the random walk) by [21]:

$$\sqrt{\left\langle R_g^2 \right\rangle} = \frac{\sqrt{\langle r^2 \rangle}}{\sqrt{6}} \quad (26)$$

For the sake of simplicity, this 'pseudo-radius-of-gyration' will be referred to as radius-of-gyration and represented by R_g.

Now it is useful to calculate the distribution function, $\Omega(R)$, associated to the density probability function, $\omega(r)$, which to our best knowledge has been overlooked in the literature. The integration of $\omega(r)$ between 0 and a distance R (i.e. to calculate the fraction of molecules for which the initial-to-end distance is smaller than R) to obtain $\Omega(R)$ is presented in Appendix I. The result is:

$$\Omega(R) = \int_0^R \omega(r)dr$$

$$= \frac{2}{\sqrt{\pi}}\left(\sum_{i=0}^{\infty}\frac{(-1)^i(BR)^{2i+1}}{i!(2i+1)} - BR\exp(-B^2R^2)\right) \quad (27)$$

Perhaps the most important feature of this function is that it depends only on the product BR with no need to consider the individual values of B and R. So, $\Omega(BR)$ is a universal curve. This characteristic is important because it makes it a general curve to be used to help solving problems in random walk and coiled polymers conformation. But why is this curve helpful to us? Because its sigmoidal shape suggests that it can be approximated by a step function (Fig. 1). A step function would mean that at each instant the initial position is surrounded by a sphere inside which it is impossible to find the fluorophore; the fluorophores have moved in this space but at that time all of them have crossed the frontier. As the time progresses the critical distance increases. There is an instant when the critical initial-to-end distance, R_{crit}, is such that it implies that the sum of volumes occupied by the molecule is a sphere of radius R_{FQ}. If this instant is close to the sensitivity limit in the time resolution of the apparatus used, then whatever is occurring inside this sphere of radius R_{FQ} can be considered instantaneous. The analogy to the

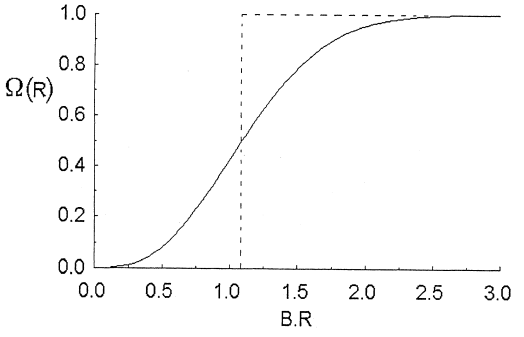

Fig. 1. The probability of finding the end position of a molecule diffusing in a random walk between distances 0 and R from the initial position (solid line) can be approximated by a step function (dashed line). The solid line is a universal curve and was plotted using Eq. 27 (see text) with 171 terms in the summation involved.

quenching sphere-of-action model is clear. Due to instrumental limitations, the overall quenching process can be divided into two phases: a static and a dynamic one.

To make our interpretation clearer, two aspects have to be made more explicit: (1) what is the instant, t_{crit}, corresponding to R_{crit}, and (2) what is the relationship between R_{crit} and the radius of the sphere that is the sum of all the volumes successively occupied by the fluorophore between instant $t=0$ and t_{crit}, R_s. The relation between these variables is depicted in Fig. 2. These two aspects will be our concern now.

For a random walk in three dimensions the elementary step length, the number of steps, the time interval and the diffusion coefficient are related by:

$$\langle r^2 \rangle = nl^2 = 6Dt \tag{28}$$

Combining Eqs. 26,28:

$$\sqrt{\langle R_g^2 \rangle} = \sqrt{Dt} \tag{29}$$

Admitting that $n \to \infty$, as before, then it is reasonable to assume that the sphere that is the sum of all the volumes successively occupied by the fluorophore is homogeneous (i.e. the density of visited places inside this sphere is constant). So it is reasonable to assume that:

$$\sqrt{\langle R_g^2 \rangle} = \sqrt{\frac{3}{5}} \langle R_s \rangle \tag{30}$$

This is a crude approximation not only because it assumes 'random coils' as homogeneous spheres but also because R_g and R_s are not monodispersed (i.e. different fluorophores have different R_g and R_s). For polydispersed systems the ratio between R_g and R_s is higher than indicated in Eq. 30 [22]. The relationship between t and R_s resulting from a combination of Eqs. 29,30 (Eq. 31) has to be considered an underestimated approximation.

$$\langle R_s \rangle = \sqrt{\frac{5}{3}Dt} \tag{31}$$

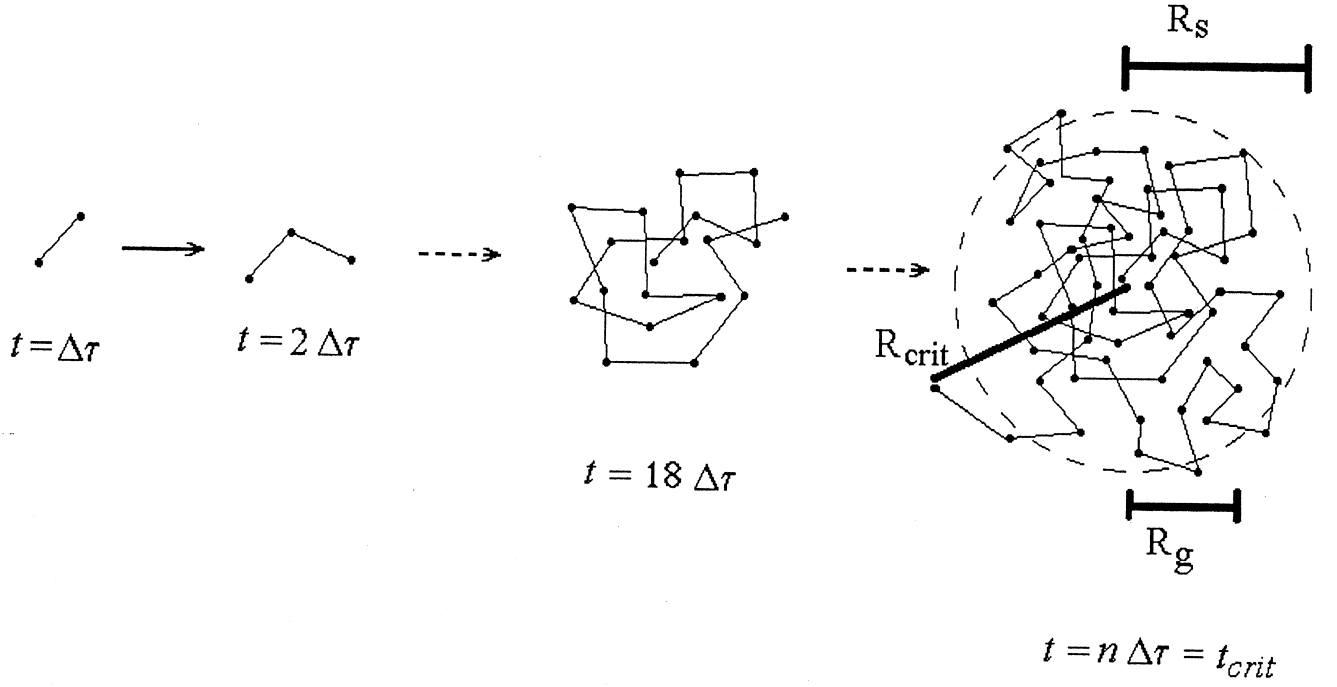

Fig. 2. Schematic representation of a random walk evolution of a molecule. The average elementary step takes time $\Delta\tau$ to occur. As the number of steps, n, goes to infinity, the steps performed by the molecule approach a random coil of global spherical geometry of radius R_s. Considering this sphere homogeneous, the radius of gyration is $R_g = 0.775R_s$. The initial-to-end distance (R) increases with time and reaches a critical value at a critical instant, t_{crit}. At this instant, R_s is equal to R_{FQ} (the sum of the molecular radii of fluorophore and quencher).

The reason why we have used the $\omega(r)$ distribution previously and are now using only average values for R_g, instead of the distribution $R_g(r)$ is explained in Appendix II and results from the fact that when $n \to \infty$, R_g is no longer dependent on r.

Several times before we have assumed that $n \to \infty$. It is now time to illustrate the applicability of this condition. We have simulated the diffusion of the ions Ca^{2+}, Cl^- and Na^+ in water (square box with 640 water molecules at constant pressure). The simulations were carried out for 100 ps and the modulus of the instantaneous velocity of each of the ions was registered with 0.25 ps intervals. To guarantee that the system was stabilized, only the last 200 registers were taken into account when calculating the average velocity. The average velocity of all the oxygen atoms of the water molecules was also calculated in the three cases. The results are depicted in Table 1. In order to calculate the mean ionic velocities, molecular dynamics simulations in explicit water were done using the GROMOS force field and suite of programs [23].

In terms of random walk model, the instantaneous velocity can be regarded as $v = l/\Delta\tau$ and

$$l = \sqrt{6D\Delta\tau}$$

(Eq. 28). Thus,

$$\Delta\tau = \frac{l^2}{6D} \tag{32}$$

$$l = \frac{6D}{v} \tag{33}$$

Considering a typical D in the order of magnitude 10^{-5} cm^2 s^{-1} and a typical $v = 0.5$ nm/ps (Table 1), we get $l = 12$ pm and $\Delta\tau = 24$ fs. These small values illustrate that the elementary steps in solution occur at time and length scales much smaller that the ones we probe (ps and nm, respectively). The processes one probes occurs for $n \to \infty$ ($n \approx 10^3$–10^6).

Table 1
Average modulus of the velocity of some ions and water from the simulation using the GROMOS package with square boxes containing one ion and 640 water molecules at constant pressure

	$\langle v \rangle$/(nm/ps)
Na^+	0.54
Cl^-	0.43
Ca^{2+}	0.39
H_2O[a]	0.61[b]

[a]Evaluated from the velocity of the oxygen atom.
[b]The same result was obtained in three simulations.

It is now the moment to return to our initial problem: what are the conditions in which the volume V' can be interpreted as V? If the time resolution of the fluorescence life-time apparatus cannot resolve what is occurring in the sub-0.5 ns range, for instance, then the phenomena occurring within a distance of $R_s = 0.9$ nm (Eq. 31, considering a typical value $D = 10^{-5}$ cm^2 s^{-1}) can be regarded as instantaneous. This is a typical value for the sum of molecular radii. This is why the quenching sphere-of-action makes sense in some cases. Viscous media (smaller D) would demand higher t to obtain a similar R_s. The whole quenching process is dynamic but the instrumental limitations enable a sometimes useful separation between 'static' (i.e. phenomena occurring in time scales below the instrumental resolution) and dynamic (i.e. phenomena occurring in time scales above the instrumental resolution) effects. The quenching sphere-of-action concept relies on this idea of instantaneous (therefore static) quenching due to molecular contact at instant $t = 0$. The time (and therefore length) scale involved makes this a useful idea to simplify the interpretation of experimental data, mainly if complex systems are involved.

It should be stressed that it is a direct consequence of Eq. 31 that the quenching sphere-of-action model is prevented if the product Dt_r differs much from 0.3 nm^2 (i.e. if $\langle R_s \rangle$ differs much from 0.7 nm, a typical value for the molecular sum of radii), where t_r is the time resolution chosen for data analysis. Trying to analyze data from complex systems with a very good time resolution is pointless because the cumulative transient effects from several sub-populations is impossible to resolve. It is preferable to start data analysis from a time where the application of the quenching sphere-of-action is meaningful, even in the case where instrumental time resolution is better than this limit. The separation between 'static' and dynamic effects is always possible but a meaningful interpretation of V is only achieved for $Dt_r \approx 0.3$ nm^2.

It should be recalled that if the quenching sphere-of-action is being properly used then the radius of the sphere of volume V is R_{FQ}. Certainly unrealistic

molecular radii could be used to define an 'effective' quenching sphere-of-action, in parallel with the radius of interaction in the radiation boundary condition, which can be very small to account for the low efficiency of the quenching process. In our opinion this should be avoided. If $\gamma < 1$ then the product γV has to be considered instead of V (Eq. 21 instead of Eq. 22).

3. Data analysis

3.1. Quenching sphere-of-action

From now on we will take advantage of the simplicity of the quenching sphere-of-action model to perform simple data analysis in complex, heterogeneous systems. Of course it will be assumed that the experimental conditions are such that this model is applicable ($Dt_r \approx 0.3$ nm^2, see above).

Imagine a simple, isolated single fluorophore for which the fluorescence intensity decay is

$$I(t) = a_0 \exp(-t/\tau_0) \tag{34}$$

This is Eq. 9 setting [Q] = 0 and $I(0) = a_0$. We consider the following quencher concentration dependence for fluorescence lifetime and pre-exponential factor, which are easily derived:

$$\frac{\tau_0}{\tau} = 1 + k_q[Q]\tau_0 \tag{35}$$

$$a = a_0 \exp(-\gamma V N_A[Q]) \tag{36}$$

Eq. 35 is the well-known Stern-Volmer plot for dynamic quenching. Eq. 36 quantifies the decrease in the pre-exponential factor due to the increase in the quencher concentration [20]. This reflects the decrease in the fluorescence intensity at instant $t = 0$ (in reality, faster than the time resolution of the apparatus in use, as explained before) due to the increasing probability of having quencher molecules in contact with the fluorophores. The intensity decay is then described by the very simple Eq. 37 instead of the rather complex Eq. 9.

$$I(t) = a_0 \exp(-\gamma V N_A[Q]) \exp(-t/\tau) \tag{37}$$

Moreover, if there are several independent sub-populations of fluorophores, the total fluorescence decay is simply:

$$I(t) = \sum_i a_{0,i} \exp(-\gamma V N_A[Q]_i) \exp(-t/\tau_i) \tag{38}$$

Usually V and γ can be considered constant (i.e. not to depend on i) and therefore are not referred to as V_i and γ_i, respectively. The steady-state Stern-Volmer plot is

$$\frac{I_{f,0}}{I_f} = \frac{\sum_i a_{0,i}\tau_{0,i}}{\sum_i (a_{0,i} \exp(-\gamma V N_A[Q]_i)\tau_i)} \tag{39}$$

It should be stressed that Eq. 39 is an approximation. The decrease in amplitude accounts for most of the transient effect, except for a small contribution at very early times (see Fig. 3). This contribution can be safely ignored in most experimental conditions.

The appearance of a new and fast component in the fluorescence intensity decay with the increase in [Q] (the previously described transient term) has been clearly experimentally detected by Nemzek and Ware [10] using time domain techniques and by Lackowicz [24] using frequency domain techniques. While this is to be expected from Eq. 9, at first glance it looks unexpected from Eq. 38. This is a consequence of the adoption of the quenching sphere-of-action model. The transient effects (i.e. the fast processes) are regarded as instantaneous.

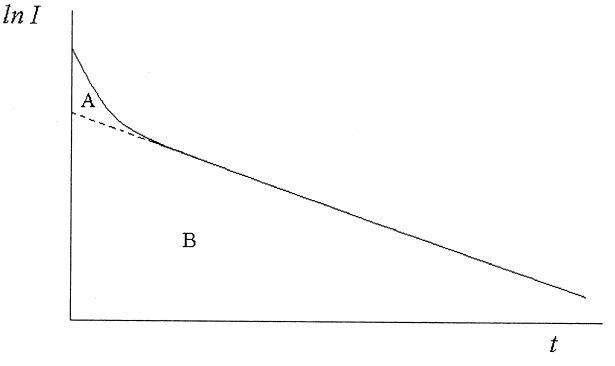

Fig. 3. Fluorescence intensity decays may be integrated and the result compared to the data directly obtained in steady-state experimental conditions. Ignoring transient effects (i.e. the linearity deviation depicted in the figure) introduces the error of neglecting area A relative to the total area A+B. The contribution of area A can be safely ignored in most experimental conditions.

3.2. Static quenching by ground-state complexation

If the fluorophore, F, and quencher, Q, associate in the ground state forming non-fluorescent complexes, FQ, then true static quenching occurs (i.e. non-diffusive). The system is described by the association constant, K_a, which in the case of 1:1 stoichiometry is

$$K_a = \frac{[FQ]}{[F][Q]} \tag{40}$$

Assuming experimental conditions that render $I_f \propto [F]$, i.e.

$$I_f = m[F] \tag{41}$$

where $m = 2.303 G\varepsilon\phi l I_0$ (G is an instrumental factor dependent on the geometry of the system, ϕ is the fluorescence quantum yield, l is the light path, ε is the molar absorptivity and I_0 is the incident light intensity). From Eqs. 40,41 it is concluded that

$$\frac{I_{f,0}}{I_f} = 1 + K_a[Q] \tag{42}$$

Nevertheless, [Q] is a difficult to handle variable, unless the approximation $[Q] \approx [Q]_t$ is valid ($[Q]_t$ is the total quencher concentration; $[Q]_t = [Q] + [FQ]$). This only occurs for a limited range of small and moderate K_a, except for very high quencher concentration where $[Q]_t \gg [F]$. A more general and useful equation can be deduced from the combination of Eqs. 40–42:

$$\frac{I_{f,0}}{I_f} = 1 + \frac{mK_a}{I_f K_a + m}[Q]_t \tag{43}$$

Combining Eqs. 40,41,43:

$$\frac{I_{f,0}}{I_f} = 1 + \frac{K_a}{\frac{[FQ]}{[Q]} + 1}[Q]_t \tag{44}$$

If $[FQ] \ll [Q]$ then Eq. 44 can be simplified to Eq. 45, which is the 'classical' equation to analyze static quenching Stern-Volmer plots. The general equation (Eq. 44) and underlying limitations to the use of Eq. 45 have been frequently overlooked in the literature.

$$\frac{I_{f,0}}{I_f} = 1 + K_a[Q]_t \tag{45}$$

It is commonly believed that an upward curvature in the steady-state Stern-Volmer plot indicates the conjugation of static and dynamic effects in quenching. Eq. 43 demonstrates clearly that pure static quenching by complexation also leads to upward curvatures in Stern-Volmer plots. Only if $[FQ] \ll [Q]$ can this intrinsic curvature be ignored. For pure dynamic quenching an upward curvature is also expected from the transient effects (the pseudo-static effects in the quenching sphere-of-action).

For transient-state data analysis we will assume once more that Eq. 34 is valid for a simple, isolated and single fluorophore. The pre-exponential factor is not proportional to the total number of fluorophores in solution, but to the number of free fluorophores in solution. However, admitting that $[Q] \approx [Q]_t$ (i.e. K_a is small enough and Eq. 45 is valid)

$$a \propto [F] = \frac{[F]_t}{1 + K_a[Q]_t} \tag{46}$$

So

$$a = \frac{a_0}{1 + K_a[Q]_t} \tag{47}$$

The fluorescence intensity decay of several sub-populations of these chromophores is

$$I(t) = \sum_i \frac{a_{0,i}}{1 + K_a[Q]_{t,i}} \exp(-t/\tau_i) \tag{48}$$

(assuming that $[Q]_t$ and K_a are constant for all subpopulations) and the steady-state Stern-Volmer plot is

$$\frac{I_{f,0}}{I_f} = \frac{\sum_i a_{0,i}\tau_{0,i}}{\sum_i \left(\frac{a_{0,i}}{1 + K_a[Q]_{t,i}} \tau_i \right)} \tag{49}$$

If no dynamic (i.e. diffusion dependent) quenching is occurring at all, then τ_i is independent of $[Q]_t$ and so $\tau_i = \tau_{0,i}$.

3.3. Final remarks on data analysis

It is artificial to make a clear separation between static and dynamic quenching. Imagine the quenching sphere-of-action model with an alteration: instead of using Poisson statistics to calculate the probability of finding at least one quencher inside the sphere of action, an interaction energy between F

and Q is used. The Q distribution around F is no longer random and takes into account an association between F and Q in the ground state. From this point of view the quenching sphere-of-action model is just a limit for static quenching, as described previously by others (e.g. [7]). This becomes clear if one recalls that $\exp(x) \approx 1+x$ when x is small enough. For small enough $K_a[Q]_t$, $1+K_a[Q]_t$ is approximately $\exp(K_a[Q]_t)$ which is equal to the quenching sphere-of-action expression, $\exp(VN_A[Q]_t)$, setting $K_a = VN_A$. In fact, Andre et al. [25] in addition to the transient contribution in Eq. 9 included a purely static exponential term such as the one of the quenching sphere-of-action formulations. Szabo [26] predicted that a distant dependent bimolecular reaction rate would result in the occurrence of static quenching, leading to an additional exponential factor to the Stern-Volmer equation derived by Nemzek and Ware.

A further problem consists in the definition of quencher concentration (e.g. in Eqs. 39,49) in heterogeneous systems. If the quencher has a restricted accessibility to the fluorophore, this effect can be accounted for in the use of local concentrations, instead of global averaged concentrations. This was recently applied to the quenching of a fluorescent probe incorporated in a model system of membranes [27]. The local quencher concentration, $[Q]_{loc}$, is considered to be related to the global average concentration, $\langle[Q]\rangle$, by:

$$[Q]_{loc} = \rho\langle[Q]\rangle \quad (50)$$

ρ is introduced to account for the fact that in the micro-heterogeneous systems the quencher molecules may not be distributed homogeneously relative to fluorophores. However, this is not as straightforward as it seems due to the possible implications of heterogeneity in D_{FQ}. To elucidate this question is one of the goals of this work.

3.4. Examples of experimental data analysis

Eq. 38 or Eq. 48 can be used to simultaneously analyze a set of fluorescence decays. A series of decays, each one obtained with a different quencher concentration, can be correlated in a global analysis so that V (Eq. 38) or K_a (Eq. 48) can be calculated from transient-state fluorescence data. Eq. 38 is a limit of Eq. 48 for weak fluorophore-quencher interactions. The steady-state data (e.g. Stern-Volmer plots) are related to transient-state data by means of Eqs. 39,49. If good estimates of V and K_a are obtained from Eq. 38 or Eq. 48, experimentally measured Stern-Volmer plots should be in agreement to those predicted by Eq. 39 or Eq. 49, respectively. This methodology has been applied before [20,28]. A fluorophore (pentaene) incorporated in a model system of membranes has a complex decay (two components) [28]. Using this methodology, it was possible to clearly separate the effect of quenching in each of them separately and check the self-consistency of the results by comparing the experimental Stern-Volmer plots with the ones from Eqs. 39,49. Eq. 49 was used when Eq. 39 failed to reproduce the data with a V value having a physical meaning. V must correspond to a radius which is related to molecular contact ($R_s \approx R_{FQ}$). In general, this methodology made it possible to ascribe a specific in-depth location inside the lipid bilayer to each component in the fluorescence decay. In another study [20], the complex fluorescence decay (three components) of an aggregate in aqueous solution was studied using this methodology. The results pointed to an open structure since none of the components was completely protected from aqueous quencher agents.

4. Interpretation of results

According to the previous section, the fluorescence decays of chromophores having several sub-populations can be analyzed using Eqs. 38,48. These equations should lead to the following results, necessary for a self-consistent set of results and interpretation:

1. The lifetime components for each sub-population must vary with the quencher concentration according to linear Stern-Volmer plots (i.e. $\tau_{0,i}/\tau_i$ vs. [Q]), unless concentration-dependent quencher aggregation is occurring [28]. Eq. 6 is then used to obtain information on the dynamics of each sub-population.
2. The reconstitution of the steady state Stern-Volmer plot using Eqs. 39,49 must agree with the experimental Stern-Volmer plot measured in steady state conditions.

3. The volume V must correspond to the radius R_{FQ}.

It should be stressed that the data for the different quencher concentrations should be globally analyzed [29]. We shall now focus on the reasons why the steady-state Stern-Volmer plot may not be linear and how to rationalize such deviations to linearity by means of Eqs. 39,49. If all the components have identical quenching properties (i.e. K_{SV}, γ, local [Q] and V or K_a) then the steady-state Stern-Volmer plot is linear with intercept 1 and slope K_{SV}. Non-linearities arise from differential quenching properties between the components. V (i.e. R_{FQ}) or K_a and γ can be regarded as intrinsic properties, i.e. depending only on the spectroscopic characteristics of fluorophore and quencher, so we turn to the local [Q] around each component i ($[Q]_i$) and their diffusion coefficients, $D_{FQ,i}$, (i.e. the local viscosity in their environments) to relate the Stern-Volmer plot linearity deviations to the physical properties of the system understudy. γ can be estimated from fluorescence quenching experiments in homogeneous solvent. Although γ is viscosity-dependent, in practical terms this dependence is not restrictive in many cases [30,31].

There are three clear limit situations from this point of view:

(1) $[Q]_i = [Q]_{i+1}$ and $D_{FQ,i} \neq D_{FQ,i+1}$, $\forall_i$

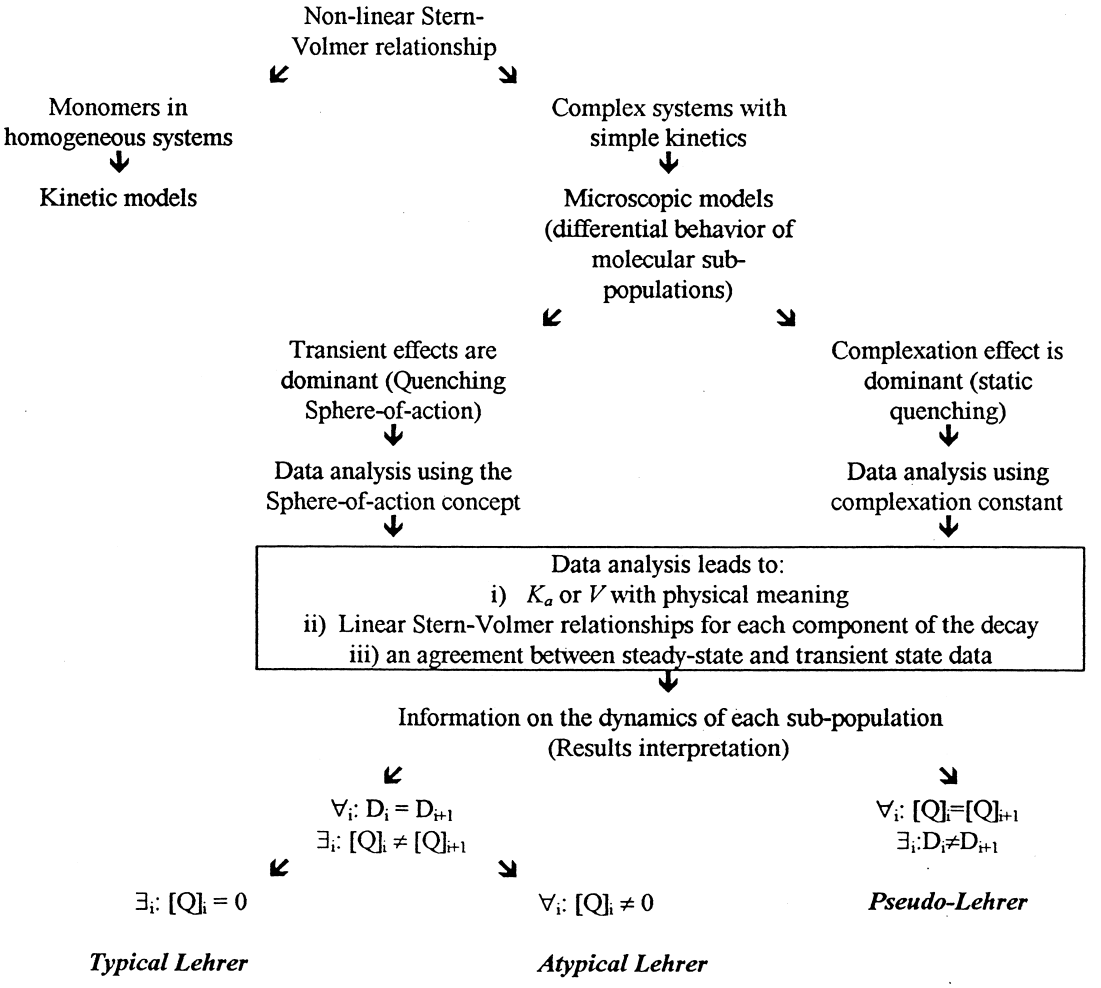

Fig. 4. Schematic sequence of steps in data analysis and results interpretation in fluorescence quenching in complex systems. This methodology enables one to overcome the difficulties imposed by the transient effects in micro-heterogeneous systems (i.e. with several sub-populations of fluorophores present).

In this case the curvature in the Stern-Volmer plot is due to the difference in the diffusive properties of the several sub-populations and is not at all related to the accessibilities of the quencher to the chromophores. We shall name this kind of situation **pseudo-Lehrer**. The plots may look like the ones studied by Lehrer [4] but for completely different reasons.

(2) $\exists_i:[Q]_i \neq [Q]_{i+1}$ and $D_{FQ,i} = D_{FQ,i+1}$, $\forall_i$

In these cases one has Lehrer-related situations because the curvature in Stern-Volmer plots is related to the accessibility of the quencher to the chromophores. Two limiting cases exist:

(2.1) $\exists_i:[Q]_i = 0$; this is a **typical Lehrer** situation.

(2.2) $\forall_i:[Q]_i \neq 0$; this is an **atypical Lehrer** situation.

The sequence in data analysis and results interpretation in fluorescence quenching experiments by means of microscopic models is depicted in Fig. 4. It should be recalled that the deviations from linearity in Stern-Volmer plots can also be explained using purely kinetic models. Complex kinetic schemes may be used to explain curvatures in the fluorescence quenching of simple systems (e.g. free monomers in homogeneous solvent) where microscopic models make no sense.

5. Conclusions

This work is especially relevant for dealing with complex systems, i.e. those where the intrinsic fluorophore decay is non-monoexponential, as is usually the case in membranes, micelles and colloidal systems. In all these cases it is not possible to statistically analyze transient effects because those belonging to different sub-populations are superimposed. Fluorescence quenching experiments in complex, heterogeneous systems may be useful and informative as long as proper and adequate data analysis and results interpretation is carried out. The use of microscopic models and a clear notion of the concept of quenching sphere-of-action and static quenching leads to very simple multi-exponential equations for transient-state data analysis. The integration of these functions leads to the expected steady-state Stern-Volmer plot. The self-consistency of the results is easily evaluated from: (1) the physical meaning of the quenching sphere-of-action volume, which has to correspond to a radius equal to the distance of closest approach, or, alternatively, from the fluorophore-quencher association equilibrium constant, (2) from the linearity in the transient-state Stern-Volmer plot for each sub-population of chromophores, and (3) from the agreement between expected steady-state Stern-Volmer plots from transient state and directly measured fluorescence data in steady state. Moreover, this kind of approach makes it possible that sets of self-consistent results can be grouped according to the reason why steady-state Stern-Volmer plots may deviate from linearity. Linearity deviations may be related to: (1) the diffusion properties of quencher and/or fluorophore, (2) the local concentration of the quencher around the fluorophore. The first reason is not at all related to the reasons previously studied by Lehrer [4] who related downward curvature in Stern-Volmer plots to the lack of accessibility of the quencher to a fraction of the fluorophores. It is therefore a 'pseudo-Lehrer' situation. The second reason is related to Lehrer's studies. If for at least one fluorophore sub-population the local quencher concentration is zero (i.e. the fluorophore is not accessible to the quencher) this is a 'typical Lehrer' situation. If the local quencher concentration is different for at least one pair of sub-populations but is not zero for any of them, then this is an 'atypical Lehrer' situation.

The approximation of the transient effects by the quenching sphere-of-action model is not always possible. The quenching sphere-of-action concept can be regarded as a valuable tool only in a limited range of experimental conditions, namely time resolution.

The static quenching (involving non-fluorescent complexes between fluorophore and quencher) Stern-Volmer equation usually used for data analysis is only valid for a limited range of small and moderate equilibrium association constants, K_a, although this is frequently overlooked in the literature. A correct awareness of data analysis validity conditions is essential for meaningful results interpretation. This work explores these limitations in fluorescence quenching.

Acknowledgements

The authors wish to acknowledge Dr. Cláudio Soares for valuable help in the molecular dynamics calculations, Mr. Luís Loura and Dr. Mário Nuno Berberan-Santos for helpful critical discussions of the manuscript, and MCT-PRAXIS XXI (Portugal; Projects PECS/C/SAU/144/95 and PCNA/C/BIO/56/96) and Fundação Calouste Gulbenkian (Portugal) for financial support.

Appendix I: The initial-to-end probability distribution function in a random walk

The probability of a random walk to end at a distance between r and $r+\mathrm{d}r$ from its initial point is

$$\omega(r)\mathrm{d}r = \left(\frac{B}{\sqrt{\pi}}\right)^3 4\pi r^2 \exp(-B^2r^2)\mathrm{d}r \quad \text{(AI.1)}$$

$$B = \frac{1}{l}\sqrt{\frac{3}{2n}} \quad \text{(AI.2)}$$

where l is the length of the elementary step and n is the number of steps [21]. The probability distribution function represents the probability of the distance between the initial and final point of the random walk to be between zero and a certain value, R. This probability is

$$\Omega(R) = \int_0^R \omega(r)\mathrm{d}r = 4\pi\left(\frac{B}{\sqrt{\pi}}\right)^3 \int_0^R r^2\exp(-B^2r^2)\mathrm{d}r \quad \text{(AI.3)}$$

Our goal in this Appendix is to calculate $\int_0^R r^2\exp(-B^2r^2)\mathrm{d}r$. It is convenient to make a change of variable: $B^2r^2 = z$. So,

$$\int_0^R r^2\exp(-B^2r^2)\mathrm{d}r = \frac{1}{2B^3}\int_0^{(BR)^2} z^{3/2-1}\exp(-z)dz \quad \text{(AI.4)}$$

The integral in the second term is an incomplete gamma function [32], $\gamma(\alpha, x) = \int_0^x t^{\alpha-1}\exp(-t)\mathrm{d}t$, where α is a constant. Therefore,

$$\frac{1}{2B^3}\int_0^{(BR)^2} z^{3/2-1}\exp(-z)dz = \gamma(\frac{3}{2},\ B^2R^2)\frac{1}{2B^3} \quad \text{(AI.5)}$$

According to Davis [32]:

$$\gamma(\alpha+1, x) = \alpha\gamma(\alpha, x) - x^\alpha\exp(-x) \quad \text{(AI.6)}$$

$$\gamma(1/2, x) = \sqrt{\pi}\,\mathrm{erf}(\sqrt{x}) \quad \text{(AI.7)}$$

Transforming Eq. AI.5 according to Eq. AI.6 and then Eq. AI.7:

$$\gamma(3/2,\ B^2R^2)\frac{1}{2B^3} = \left(\frac{\sqrt{\pi}}{2}\mathrm{erf}(BR) - BR\exp(-B^2R^2)\right)\frac{1}{2B^3} \quad \text{(AI.8)}$$

Substituting erf(BR) by its series expansion [33] (Eq. AI.9) leads to the result aimed for (Eq. AI.10).

$$\mathrm{erf}(BR) = \frac{2}{\sqrt{\pi}}\sum_{i=0}^{\infty}\frac{(-1)^i(BR)^{2i+1}}{i!(2i+1)} \quad \text{(AI.9)}$$

$$\Omega(R) = \int_0^R \omega(r)\mathrm{d}r = \frac{2}{\sqrt{\pi}}\left(\sum_{i=0}^{\infty}\frac{(-1)^i(BR)^{2i+1}}{i!(2i+1)} - BR\exp(-B^2R^2)\right) \quad \text{(AI.10)}$$

Appendix II: The radius of gyration dependence on the initial-to-end distance in a random walk

In this Appendix we shall refer to the radius of gyration, R_g, of a random walk meaning the R_g that would have a polymer chain linking all the points in space visited by the moving molecule during the random walk for a period τ. It is, of course, a pseudo-radius of gyration but for the sake of simplicity we shall name it radius-of-gyration and represent it by R_g.

It is important to recall that the relation between the radius of gyration and the initial-to-end distance in a random walk is not bi-univocous, i.e. molecules

having the same R_g may not have the same initial-to-end distance and vice versa. Therefore, for each initial-to-end distance, r, there is an average R_g that we will represent by $\langle R_g\rangle(r)$. As it is more convenient to work with the squared R_g and squared initial-to-end distance, in practice $\langle R_g^2\rangle(r^2)$ is more useful to work with. The R_g averaged over all the population is constant and simply referred to as $\langle R_g\rangle$. $\langle R_g^2\rangle$ also refers to a total population average.

For a specific random walk, the R_g depends on the distance between each of the elementary steps:

$$R_g^2 = \frac{1}{(n+1)^2}\sum_{j=i+1}^{n}\sum_{i=1}^{n-1} r_{ij}^2 \qquad \text{(AII.1)}$$

(r_{ij} is the shortest distance between steps i and j). The whole process is random, so the average distance between any $j-i$ steps is the same ($\langle r_{ij}^2\rangle = (j-i+1)l^2$) and the average R_g^2 is

$$\langle R_g^2\rangle = \frac{1}{(n+1)^2}\sum_{k=1}^{n-1}(n-k)\langle r_{i,i+k}^2\rangle$$

$$= \frac{l^2}{(n+1)^2}\sum_{k=1}^{n-1}(n-k)(k+1) \qquad \text{(AII.2)}$$

Eq. AII.3 is now applied in Eq. AII.2 and the result is Eq. AII.4.

$$\sum_{i=1}^{n-1}(n-i)i = \frac{n^3-n}{6} \qquad \text{(AII.3)}$$

$$\langle R_g^2\rangle = \frac{\langle r^2\rangle n^2 + 3n - 4}{6\quad (n+1)^2} \qquad \text{(AII.4)}$$

When $n\to\infty$ Eq. AII.4 can be approximated by the very well-known relationship (Eq. AII.5) used for random coils.

$$\langle R_g^2\rangle = \frac{\langle r^2\rangle}{6} \qquad \text{(AII.5)}$$

A similar sequence is used in the deduction of $\langle R_g^2\rangle(r^2)$ with a small difference. We shall now consider the initial-to-end distance, $r = r_{1n}$, apart from the rest of the inter-step distances in Eq. AII.2:

$$\langle R_g^2\rangle(r^2) = \frac{1}{(n+1)^2}\sum_{k=1}^{n-1}(n-k)\langle r_{i,i+k}^2\rangle$$

$$= \frac{1}{(n+1)^2}\left(r^2 + \sum_{j=2}^{n-1}\langle r_{1,j}^2\rangle + \sum_{j=i+1}^{n}\sum_{i=2}^{n-1}\langle r_{ij}^2\rangle\right)$$

$$= \frac{1}{(n+1)^2}\left[r^2 + l^2\left(\frac{n+1}{2}(n-2) + \sum_{j=i+1}^{n}\sum_{i=2}^{n-1}(j-i+1)\right)\right] \qquad \text{(AII.6)}$$

Applying Eq. AII.7 and then Eq. AII.3 to Eq. AII.6 gives the result aimed for (Eq. AII.8).

$$\sum_{j=i+1}^{n}\sum_{i=2}^{n-1}(j-i+1) = \left(\sum_{k=1}^{n-1}k(n-k)\right) - (n-1) \qquad \text{(AII.7)}$$

$$\langle R_g^2\rangle(r^2) = \frac{1}{(n+1)^2}$$

$$\left[r^2 + l^2\left(\frac{3(n-2)(n+1) + n(n-1)(n+1) - 6(n-1)}{6}\right)\right] \qquad \text{(AII.8)}$$

Substituting r^2 by $\langle r^2\rangle = nl^2$ in Eq. AII.8, Eq. AII.4 is obtained, as expected.

The meaningful characteristic of Eq. AII.8 for this work is that when $n\to\infty$, the term $r^2/(n+1)^2 \to 0$; i.e. the average square radius-of-gyration loses its dependence on r and therefore becomes a constant. The constant value is $\langle R_g^2\rangle(r^2) = \langle R_g^2\rangle = \langle r^2\rangle/6 = Dt$ (R_g depends only on the diffusive properties of the molecules involved).

References

[1] S.A. Rice, in: C.H. Bamford, C.H.F. Tiffer, R.G. Compton (Eds.), Comprehensive Chemical Kinetics, Vol. 25, Elsevier, Amsterdam, 1985.

[2] W.R. Laws, P.B. Contino, Methods Enzymol. 210 (1992) 448–463.

[3] M.R. Eftink, C.A. Ghiron, Anal. Biochem. 114 (1981) 199–227.

[4] S. Lehrer, Biochemistry 10 (1971) 3254–3263.

[5] M.R. Eftink, C.A. Ghiron, J. Phys. Chem. 80 (1976) 486–493.

[6] C.S. Owen, J.M. Vanderkooi, Comm. Mol. Cell. Biophys. 7 (1991) 235–257.
[7] M.R. Eftink, in: J.R. Lakowicz (Ed.), Topics in Fluorescence Spectroscopy, Vol. 2, Plenum Press, New York, 1991.
[8] J.R. Lakowicz, Principles of Fluorescence Spectroscopy, Plenum Press, New York, 1983.
[9] R.M. Noyes, Prog. Reaction Kinet. 1 (1961) 131–160.
[10] T.L. Nemzek, W.R. Ware, J. Chem. Phys. 62 (1975) 477–489.
[11] D.D. Eads, B.G. Dismer, G.R. Fleming, J. Chem. Phys. 93 (1990) 1136–1148.
[12] R. Das, N. Periasamy, Chem. Phys. 136 (1989) 361–378.
[13] K. Razi-Naqvi, Chem. Phys. Lett. 28 (1974) 280–284.
[14] C.S. Owen, J. Chem. Phys. 62 (1975) 3204–3207.
[15] M. Almgren, in: M. Gratzel, K. Kalyanasundaram (Eds.), Kinetics and Catalysis in Microheterogeneous Systems, Marcel Dekker, New York, 1991.
[16] D.G. Truhlar, J. Chem. Educ. 62 (1985) 104–106.
[17] A. Weller, Prog. Reaction Kinet. 1 (1961) 187–212.
[18] N. Periasamy, G.C. Joshi, R. Das, Chem. Phys. Lett. 160 (1989) 457–535.
[19] F. Perrin, C.R. Acad. Sci. Paris 178 (1924) 1978–1980; 2252–2254.
[20] M.A.R.B. Castanho, M. Prieto, Eur. J. Biochem. 207 (1992) 125–134.
[21] C.R. Cantor, P.R. Schimmel, Biophysical Chemistry, Part III, The Behavior of Biological Macromolecules, W.H. Freeman and Company, New York, 1980.
[22] W. Burchard, in: H.-J. Cantow et al. (Eds.), Light Scattering from Polymers, Springer-Verlag, Berlin, 1983.
[23] W.F. van Gunsteren, H.J.C. Berendsen, Groningen Molecular Simulation (GROMOS) Library Manual, Biomos B.V., Groningen, 1987.
[24] J.R. Lackowicz, M.L. Johnson, I. Gryczynski, N. Joshi, G. Laczko, J. Phys. Chem. 91 (1987) 3277–3285.
[25] J.C. Andre, M. Niclause, W.R. Ware, Chem. Phys. 28 (1978) 371–377.
[26] A. Szabo, J. Phys. Chem. 93 (1989) 6929–6939.
[27] M. Castanho, M. Prieto, A.U. Acuña, Biochim. Biophys. Acta 1279 (1996) 164–168.
[28] M. Castanho, M. Prieto, Biophys. J. 69 (1995) 155–168.
[29] J.M. Beechem, E. Gratton, M. Ameloot, J.R. Knutson, L. Brand, in: J.R. Lakowicz (Ed.), Topics in Fluorescence Spectroscopy, Vol. 2, Plenum Press, New York, 1991.
[30] J.R. Lakowicz, H. Hogen, G. Omann, Biochim. Biophys. Acta 471 (1977) 401–411.
[31] G. Omann, J.R. Lakowicz, Science 197 (1977) 465–467.
[32] P.J. Davis, in: M. Abramowitz, I.A. Stegun (Eds.), Handbook of Mathematical Functions, Dover, New York, 1972.
[33] W. Gautschi, in: M. Abramowitz, I.A. Stegun (Eds.), Handbook of Mathematical Functions, Dover, New York, 1972.